

Protein Degradation

Discovery of a Potent Proteolysis Targeting Chimera Enables Targeting the Scaffolding Functions of FKBP51 (FKBP51)

Thomas M. Geiger[†], Michael Walz[†], Christian Meyners[†], Angela Kuehn, Johannes K. Dreizler, Wisely O. Sugiarto, Edvaldo V. S. Maciel, Min Zheng, Frederik Lermyte, and Felix Hausch*

Abstract: The FK506-binding protein 51 (FKBP51) is a promising target in a variety of disorders including depression, chronic pain, and obesity. Previous FKBP51-targeting strategies were restricted to occupation of the FK506-binding site, which does not affect core functions of FKBP51. Here, we report the discovery of the first FKBP51 proteolysis targeting chimera (PROTAC) that enables degradation of FKBP51 abolishing its scaffolding function. Initial synthesis of 220 FKBP-focused PROTACs yielded a plethora of active PROTACs for FKBP12, six for FKBP51, and none for FKBP52. Structural analysis of a binary FKBP12:PROTAC complex revealed the molecular basis for negative cooperativity. Linker-based optimization of first generation FKBP51 PROTACs led to the PROTAC SelDeg51 with improved cellular activity, selectivity, and high cooperativity. The structure of the ternary FKBP51:SelDeg51:VCB complex revealed how SelDeg51 establishes cooperativity by dimerizing FKBP51 and the von Hippel-Lindau protein (VHL) in a glue-like fashion. SelDeg51 efficiently depletes FKBP51 and reactivates glucocorticoid receptor (GR)-signalling, highlighting the enhanced efficacy of full protein degradation compared to classical FKBP51 binding.

Proteolysis targeting chimeras (PROTACs) are heterobifunctional molecules that induce the degradation of target proteins which is fundamentally different to occupying functional active sites. PROTACs contain ligands for the protein of interest (POI) and for the E3 ligase, connected through a linker. By recruiting POIs to the E3 ligase in cells, they catalytically trigger ubiquitination and subsequent degradation of the POI.^[1] One of the key prospects of PROTACs over classical inhibitors is the ability to exploit non-functional binding sites in POIs.^[2–5] The FK506-binding protein 51 (FKBP51) is a cochaperone in the Hsp90 machinery and a key regulator of steroid hormone signalling.^[6] Especially in the context of the glucocorticoid receptor (GR), FKBP51 acts in an ultra-short feedback loop to counteract the hypothalamic-pituitary-adrenal axis activation and fine-tune the stress response.^[7] In recent years, FKBP51 emerged as a promising drug target for stress-related mental disorders,^[8,9] chronic pain,^[9–13] and obesity.^[14–17] Historically, FKBP51 targeting strategies have relied on the FK506-binding site occupation but failed to address FKBP51's scaffolding function. Photo-crosslinking^[18] and cryo-EM studies^[19] of the FKBP51:Hsp90:GR complex recently demonstrated that the FK506-ligand binding site is not essential for GR regulation, explaining the limited cellular efficacy of FK506 analogues. We therefore explored if targeted FKBP51 degradation could overcome the limitations of FKBP51 occupation-based strategies.

Towards this aim, we generated 220 different FKBP-focused PROTACs by combinatorically connecting 15 different FKBP ligands, five different linker lengths ($n=1–5$, PEG-based), and three E3 ligase ligands for the von Hippel-Lindau protein (VHL) and cereblon (CRBN) (2x VHL-based, 1x CRBN-based, Figure 1). We first preassembled azide-functionalized linkers with the E3 ligase ligands (Figure 1B). These were then coupled to alkyne-functionalized FKBP ligands by copper-catalyzed click chemistry. We chose SAFit-like^[20,21] and bicyclic [4.3.1]-sulfonamide^[22–24] scaffolds as FKBP ligands due to their potency and well-understood binding mode (Figure 1A). Together, these scaffolds provided a wide range of exit vectors to explore different FKBP:VHL/CRBN orientations. All PROTAC candidates were screened for FKBP binding (Figure S1.1), cooperative ternary complex formation^[25]

[*] T. M. Geiger, M. Walz, Dr. C. Meyners, A. Kuehn, J. K. Dreizler, W. O. Sugiarto, Dr. E. V. S. Maciel, Dr. M. Zheng, Prof. Dr. F. Lermyte, Prof. Dr. F. Hausch
 Department of Chemistry and Biochemistry Clemens-Schöpfung-Institute, Technical University Darmstadt
 Peter-Grünberg-Straße 4, 64287 Darmstadt (Germany)
 E-mail: felix.hausch@tu-darmstadt.de

Prof. Dr. F. Hausch
 Centre for Synthetic Biology, Technical University of Darmstadt
 64283 Darmstadt (Germany)

[†] These authors contributed equally to this work.

© 2023 The Authors. Angewandte Chemie International Edition published by Wiley-VCH GmbH. This is an open access article under the terms of the Creative Commons Attribution Non-Commercial License, which permits use, distribution and reproduction in any medium, provided the original work is properly cited and is not used for commercial purposes.

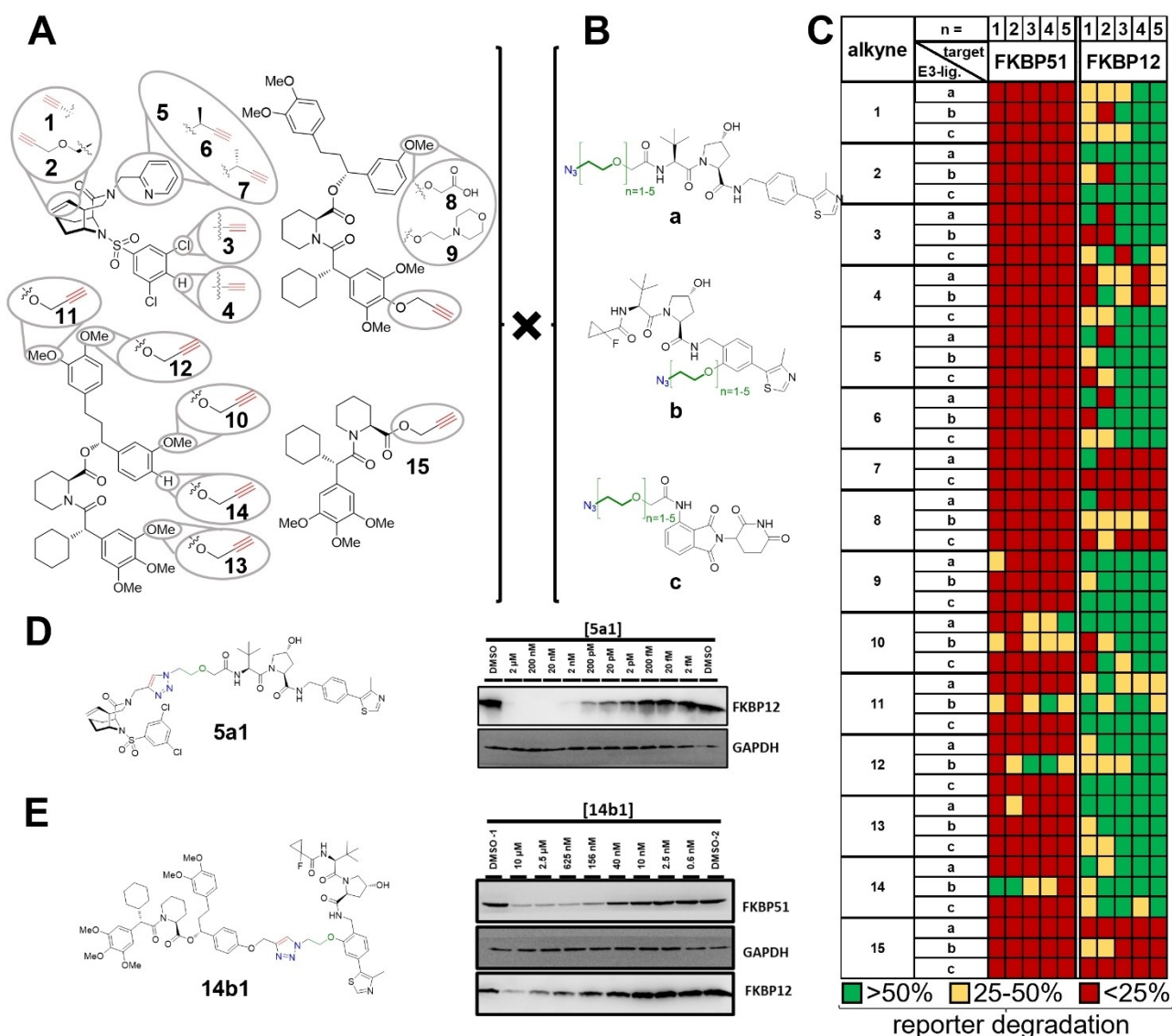


Figure 1. Overview and Design of FKBP PROTACs. A) Structures of alkyne-functionalized FKBP ligands. B) Structures of azide-functionalized linker-E3 ligase ligand building blocks. C) Degradation activity profile in FKBP51-eGFP and FKBP12-eGFP reporter assays (green: > 50% reporter degradation; yellow: 50–25% reporter degradation; red < 25% reporter degradation after 48 h treatment). D) Structure of PROTAC 5a1 and western blot of 5a1-dependent FKBP12 degradation (24 h treatment). E) Structure of PROTAC 14b1 and western blot of 14b1-dependent FKBP12 and FKBP51 degradation (24 h treatment). Uncropped western blot images are depicted in Figure S5.1.

(Figure S1.2), which describes enhanced (positive) or reduced (negative) PROTAC binding to one protein in presence of the second protein, and for degradation activity in FKBP51_eGFP and FKBP12_eGFP level reporter assays in HEK293T cells (Figure 1C & S1.3). Preliminarily active PROTACs were then validated by Western Blot for degradation of endogenous FKBP12 (Figure 1D and S1.5) and FKBP51 (Figure 1E and S1.4). Strikingly, we found that the majority of PROTACs efficiently degrade FKBP12 but only a small fraction was active for FKBP51 (Figure 1C), and none showed activity for FKBP52 (Fig S1.6 & S1.7). For FKBP51, only SAFit-based ligands yielded active PROTACs (partially explaining the lack of FKBP52 PROTACs), and there was a clear preference for VHL ligand b (Figure 1B), similar to previously reported observations for

Brd7/9 dual degraders.^[26] In contrast, activity was not limited to any E3 ligase ligand, linker length or POI attachment points for FKBP12 PROTACs. Despite the strong preference of SAFit-type ligands to recruit FKBP51 over FKBP12, all initial FKBP51 PROTACs retained substantial FKBP12-degrading activity.

Among the most potent, efficacious and selective FKBP12 PROTACs were compounds of the 5a and 6a series (Figure 2A and S2.1 & S2.2), e.g. 5a1 and 6a2 which completely (> 95 %) degraded endogenous FKBP12 with a DC_{50} = 20 pM (Figure 1D, Fig S1.5, S2.1 C & S2.1D, S2.2). Striking outliers in these series were PROTACs 5a2 and 6a2 with a linker length of $n=2$, which were completely degradation-inactive (Figure 2A and S2.1 C & S2.1D). This was not due to lack of FKBP12 (Figure 2B and S2.1E) or

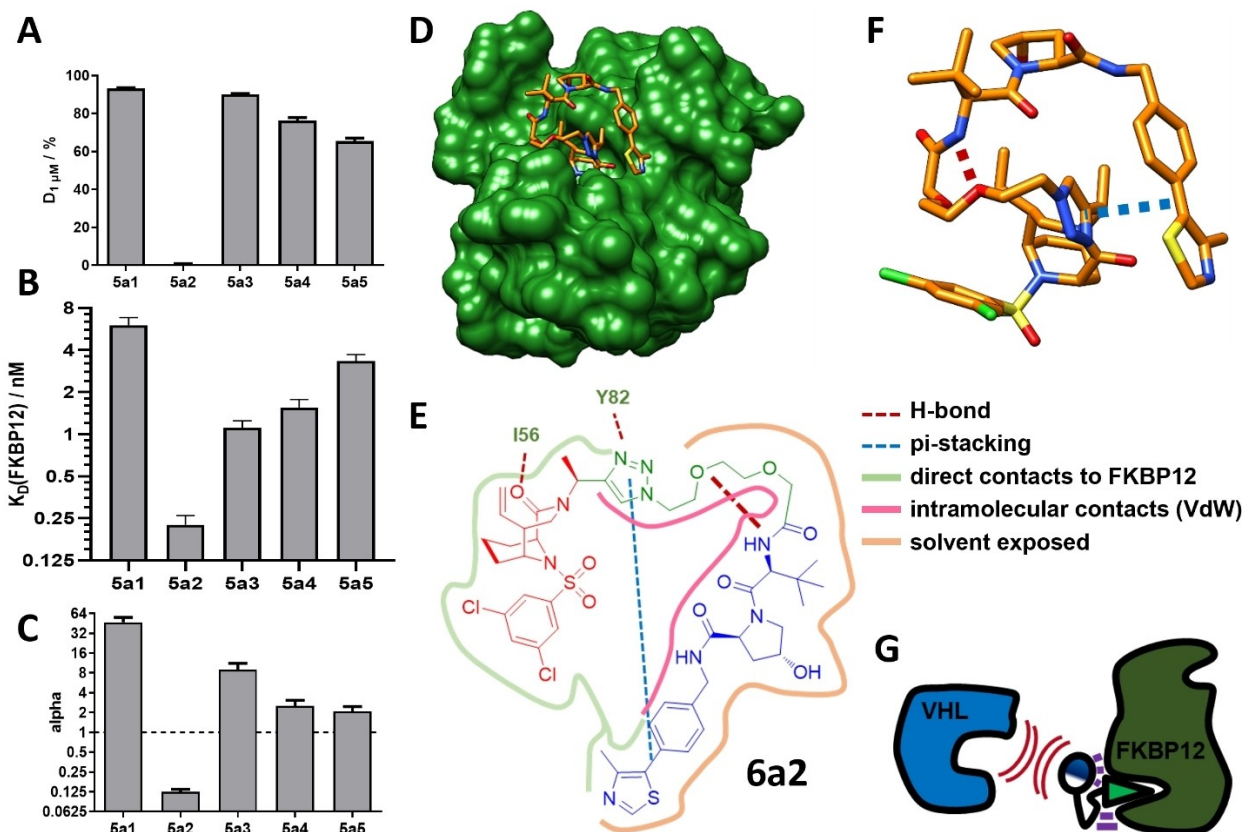


Figure 2. Crystal structure of a binary FKBP12-PROTAC complex reveals the structural basis for negative cooperativity. A) FKBP12_eGFP reporter degradation after 48 h treatment at 1 μM PROTAC. Bars and error bars represent mean and standard deviation of biological duplicates B) Binding affinities to FKBP12 derived from competitive FP assays using a FKBP-FP-tracer. Bars and error bars represent mean and standard deviation of duplicates C) Cooperativity ($\alpha = K_D(\text{binary})/K_D(\text{ternary})$) for binding to VCB derived from competitive FP assays using a VHL-FP tracer. Bars and error bars represent mean and standard deviation of triplicates D) Crystal structure and E) ligand interaction map of 6a2 bound to FKBP12. The FKBP12-binding part of 6a2 is shown in red, the VHL-binding part in blue, and the linker is colored in green. F) Conformation and intramolecular interactions of 6a2 bound to FKBP12. G) Schematic model of negative cooperativity for 5a2 and 6a2.

VHL binding (Figure S2.1F). In contrast, compounds 5a2 and 6a2 were among the most potent FKBP12 ligands reported so far,^[22,24] and bound FKBP12 substantially better than their degradation-active analogues 5a1, 5a3–5, 6a1, and 6a3–5. However, affinities to VHL of 5a2 and 6a2 were dramatically reduced in the presence of FKBP12, indicating pronounced negative cooperativity, whereas PROTAC 5a1 and other analogues displayed highly positive cooperativity (Figure 2C, S2.1G and Table S1). To elucidate the molecular basis for the negative cooperativity, we solved the crystal structure of 6a2 in complex with FKBP12 (Figure 2D). This revealed a pronounced collapse of the VHL-binding moiety of 6a2 onto the FKBP12-binding moiety, driven by an intramolecular hydrogen bond, π stacking and extensive intramolecular hydrophobic contacts (Figure 2E & 2F). Several contacts of the linker and VHL-moiety with FKBP12 were observed, explaining enhanced FKBP12 binding of 6a2 compared to the starting FKBP12 ligand. Moreover, the collapsed conformation prevents binding to VHL, explaining the observed negative cooperativity and lack of degradation activity (Figure 2G).

To improve the cellular efficacy and selectivity for FKBP51 degradation, we first characterized the binding properties of the initial PROTAC hits for binding to FKBP51 and VHL as well as cooperativity, and ternary complex formation. All initial hits retained affinity to FKBP51 and VHL. Based on the promising positive cooperativity (Table 1 & Table S2) and slight preference for degradation of FKBP51 over FKBP12 (Figure 1E), we chose 14b1 as initial starting point for optimization. Branching methylation of the linker slightly reduced degradation efficacy (Figure S3.1), whereas elongating the linker by one

Table 1: Binding affinities and cooperativities of 14b1 and SelDeg51 binding to FKBP51^{FKI}. Binding constants (in nM \pm SD) represent three replicates and were determined in a competitive HTRF assay using a FKBP-HTRF tracer either with the PROTAC alone or in presence of an excess (5 μM) of VCB.

PROTAC	$K_D(\text{PROTAC})/\text{nM}$	$K_D(\text{PROTAC:VCB})/\text{nM}$	α
14b1	26 \pm 3	0.81 \pm 0.06	32
SelDeg51	18 \pm 2	0.78 \pm 0.07	23

carbon as in SelDeg51 (Selective Degradator of FKBP51) improved potency ($D_{\max}=90\%$), efficacy and selectivity compared to 14b1 (Figure 3A & B, Figure S3.2). SelDeg51 retained high positive cooperativity for FKBP51 and potently induced ternary complex formation (Figures 3C & S3.3B, Table 1).

The molecular basis for the positive cooperativity became apparent with the crystal structure of the ternary FKBP51-SelDeg51-VHL complex (Figure 3D). The VHL and FKBP ligands are both bound to their respective binding pockets, while the linker was largely solvent-exposed (Figure 3D & E). The 2-fluoro-2-cyclopropyl moiety of the VHL ligand part of SelDeg51 is deeply buried between the two proteins, explaining the strong preference of FKBP51 for PROTACs based on VHL building block b (Figure 3E & G). We observed minor direct contacts between FKBP51 and VHL, e.g. FKBP51^{G84}:VHL^{R69},

FKBP51^{Y113,S118}:VHL^{P71}, and FKBP51^{L119,P120}:VHL^{D143,G144} (Figure 3F). Strikingly, we observed a major interaction interface between the FKBP51 ligand and VHL^{R69,P71,Q73,H110,Y112} (Figure 3G), burrowing an area of 206 \AA^2 which is in the same range as previously observed protein-protein interactions.^[27] In addition, the VHL ligand engages in direct interactions with G84 and Q85 of FKBP51 (Figure 3H). Ion mobility measurements suggested that the conformation of the ternary complex observed in the crystal structure is maintained in solution (Figure S3.3). The positive cooperativity of SelDeg51 is thus driven by a molecular glue-like binding mode that is established by extensive interactions of the FKBP- and VHL ligand parts of SelDeg51 with their originally non-cognate protein partners.

To establish SelDeg51 as a useful chemical tool, we characterized its properties in mammalian cells. SelDeg51 engaged FKBP51 in living cells, although approx. ten-fold

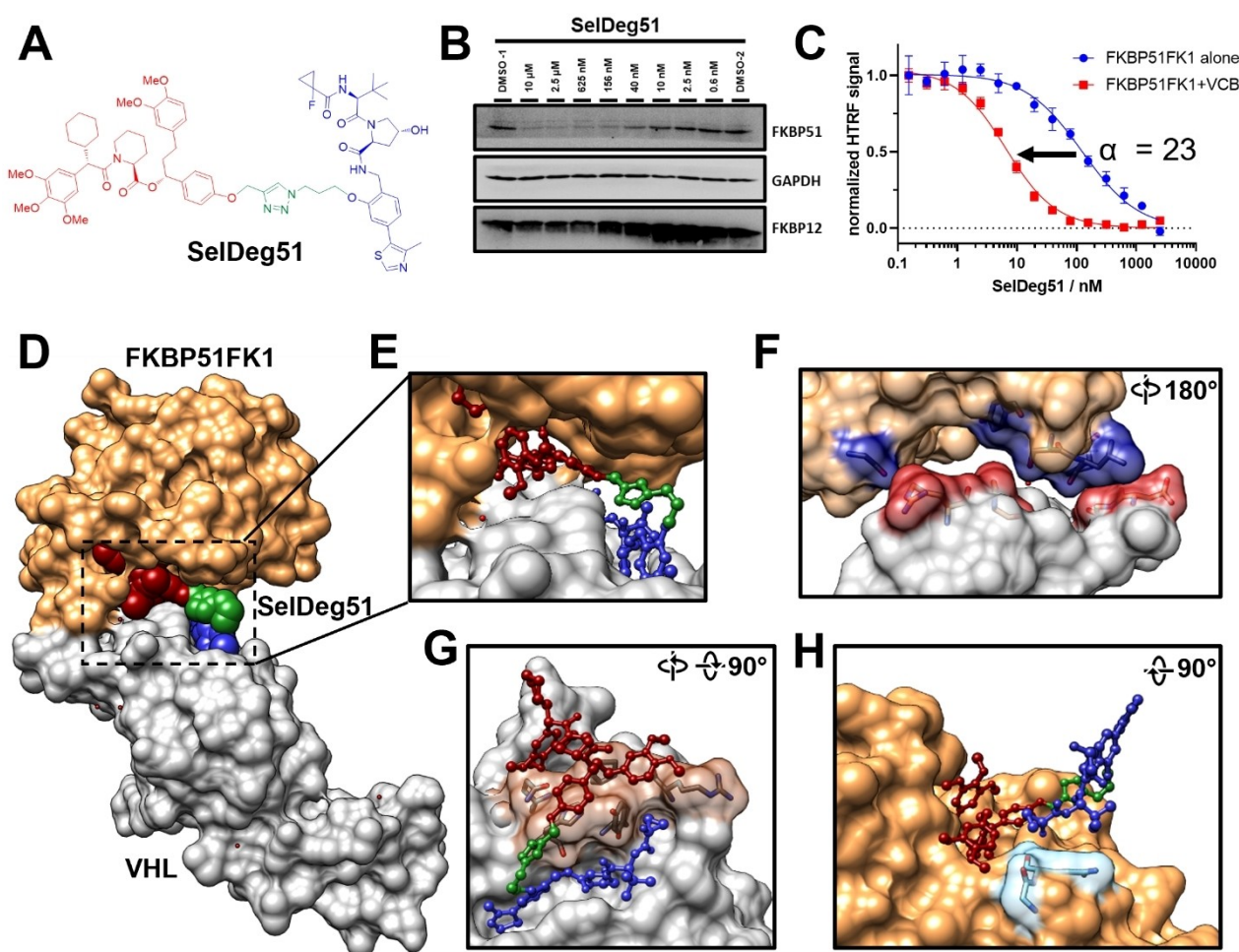


Figure 3. Identification and binding mode of SelDeg51. A) Chemical structure of SelDeg51 (red: FKBP ligand; green: linker; blue: VHL ligand). B) SelDeg51-mediated FKBP51 and FKBP12 degradation after 24 h treatment. C) SelDeg51 binding to FKBP51 in presence or absence of VCB in competitive HTRF assays using a FKBP-HTRF tracer. Symbols and error bars represent mean and standard deviation of triplicates D) Crystal structure of the ternary FKBP51-SelDeg51-VHL complex (brown: FKBP51 FK1 domain; SelDeg51 represented as spheres: red: FKBP ligand; green: linker; blue: VHL ligand; grey: VHL). E) Solvent exposed linker (green sticks) of SelDeg51. F) Direct FKBP51:VHL contacts, highlighting FKBP51 residues (blue) and VHL residues (pale red surface) in contact with the FKBP-ligand of SelDeg51 (red sticks). H) FKBP51 residues (cyan) in contact with the VHL ligand of SelDeg51 (blue sticks). Uncropped western blot images are depicted in Figure S5.2

less efficient than its precursor SAFit2 in competitive NanoBRET assays (Figure S4.1). It displayed a rather slow degradation rate and achieved maximal FKBP51 degradation after 24 hours (Figure 4A), which was reversible after 24 hours of washout (Figure 4B). To study fast FKBP51-dependent processes in cells, further optimization might be necessary to enhance the degradation rate. These results are in line with protein turnover previously reported for FKBP51.^[28] SelDeg51-induced FKBP51 degradation was blocked by the selective FKBP51 ligand 64a^[21] and the pan-selective FKBP ligand 18^(S-Me)^[24] (Figure 4C) as well as by inhibition of VHL, neddylation or the proteasome (Figure 4D & Figure S4.4). Quantitative proteomics confirmed FKBP51 as the strongest and most significantly SelDeg51-downregulated protein in MOLT-4 cells (Figure S4.2).

FKBP51 is a key regulator of the glucocorticoid receptor (GR), which is thought to contribute to stress-related disorders (such as depression),^[29] obesity,^[14] or chronic pain states.^[10–13,15,17,30] The structural basis for GR regulation by FKBP51 was recently revealed by cryo-EM^[19] and large-scale in-cell photo-crosslinking.^[18] These studies strikingly

showed that the FK506-binding site of FKBP51 is not directly involved in GR regulation. In line with these results, occupancy of the FK506-binding site by the FKBP ligand 18^(S-Me)^[24] did not affect GR signalling in HeLa cells (Figure 4E). In contrast, SelDeg51 but not its inactive control (Figure S4.3), was able to enhance GR signalling in an FKBP51-dependent manner (Figure 4E). Remarkably, the effect of SelDeg51 was abolished by an excess of ligand 18^(S-Me) (Figure 4E). To further explore the efficacy of SelDeg51 in a physiologically more relevant setting, we referred to A549 cells, a cellular model for anti-inflammatory effects of glucocorticoids.^[31] In these cells, SelDeg51 increased the Dexamethasone-induced expression of the endogenous GR target genes *GILZ* and *FKBP5* (Figure 4F), reflecting the removal of FKBP51-mediated repression of GR signalling. *FKBP5*, the gene encoding FKBP51, is one of the most prominent GR target genes, resulting in a physiologically relevant ultra-short feedback loop controlling GR responsiveness. Breaking this feedback is thought to be crucial to interfere with FKBP51's function. In contrast to SelDeg51, the potent FKBP51 ligand 18^(S-Me) did not

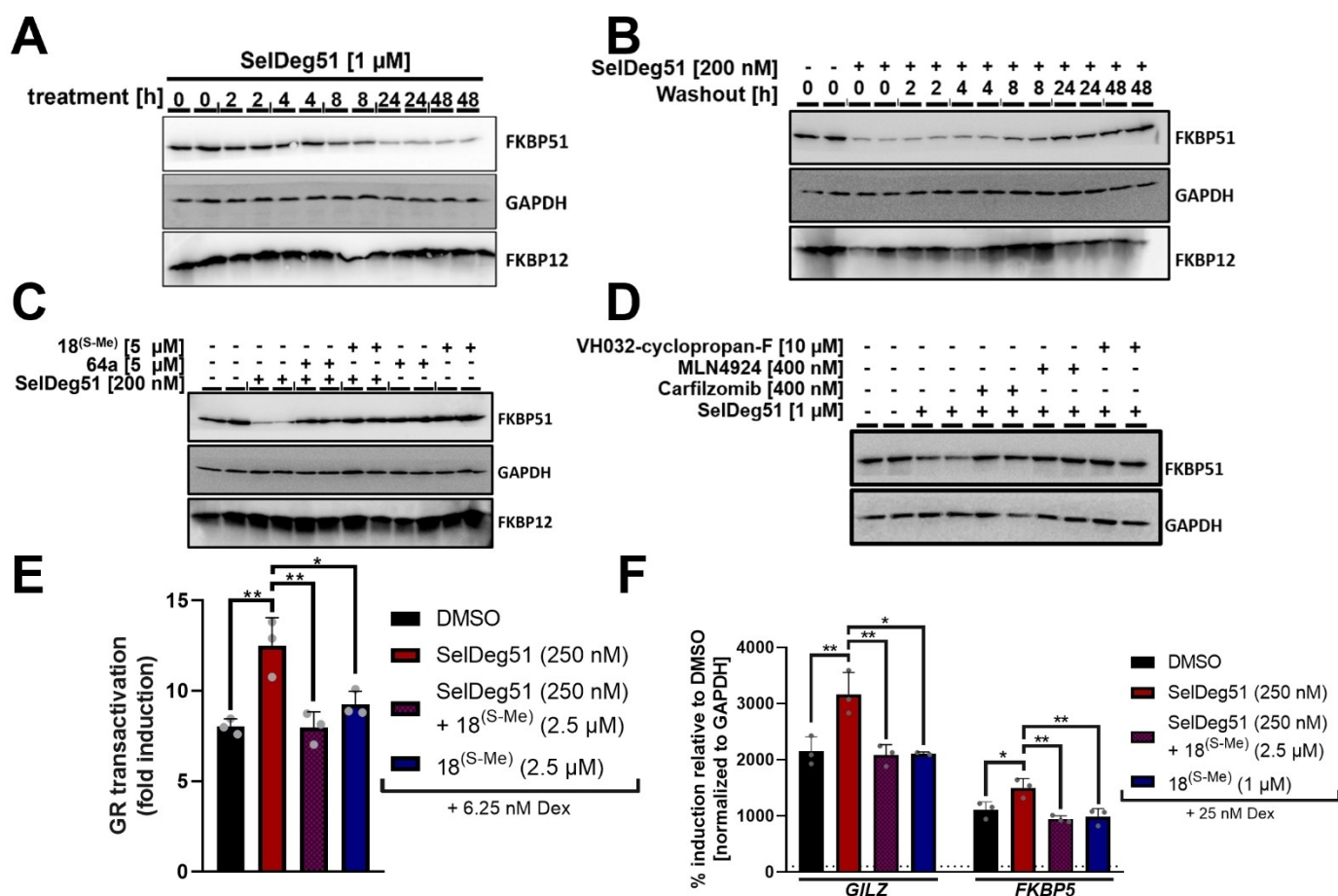


Figure 4. Cellular characterization of SelDeg51. A) FKBP51 and FKBP12 degradation kinetics of SelDeg51 in HEK293T cells. B) Persisting effects of SelDeg51 after washout. C) FK506-binding site and D) VHL as well as proteasome-dependent mode of action. E) SelDeg51 (250 nM) mediated FKBP51 degradation but not FKBP ligands (2.5 μM) reactivate GR-signalling in GR reporter gene assays in HeLa cells. Bars and error bars represent mean and standard deviation of three replicates. F) SelDeg51-mediated FKBP51 degradation but not FKBP ligands stimulates endogenous GR-controlled *GILZ* and *FKBP5* expression in A549 cells, determined by qPCR. Bars and error bars represent mean and standard deviation of at least 2 technical replicates. Uncropped western blot images of A)–D) are depicted in Figure S5.3.

affect Dex-stimulated *GILZ* or *FKBP5* mRNA expression. However, FKBP51 binding site occupancy by 18^(S-Me) prevented the effect of SelDeg51, strikingly underscoring the superiority of FKBP51 degradation vs FKBP51 occupancy.

In summary, we here present SelDeg51 as the first efficacious FKBP51 PROTAC and unique tool to target the scaffolding functions of FKBP51. SelDeg51-mediated degradation but not FK506-binding site occupation reactivated GR signalling, providing a pharmacological tool to revert FKBP51-mediated stress hormone receptor suppression. Relative orientation of POI and E3 ligase and cooperativity are known key parameters for PROTAC development^[3,25,32] that remain poorly understood in many cases. Our results show how the fine-tuning of (non-cognate) PROTAC-protein contacts can overcome a strong adverse degradability bias among close homologs (e.g. 125 active PROTAC hits for FKBP12 vs. 6 for FKBP51). We reveal a molecular glue-like ternary complex for SelDeg51 and provide the structural basis for negative cooperativity by hyper-affinity FKBP12 PROTACs. The ability to utilize non-functional binding sites is a unique potential asset of PROTACs but clear examples for this are rare,^[2-5] likely due to the scarcity of truly neutral recruiting ligands. Our results provide the proof-of-concept for a mechanistically new approach to target FKBP51, providing a basis for the development of more efficacious FKBP51-directed drugs.

Acknowledgements

The authors thank Tianqi Mao, Andreas Hähle and Horst W. Schuchmann for their preliminary results working on FKBP-PROTACs. We thank Ahmed Bulldan and Alexander Löwer for their help with qPCR experiments. We thank Katherine A. Donovan, Eric S. Fischer and the Fischer Lab Degradation Proteomics Initiative for collection of the global proteomics data supported by NIH CA214608 and CA218278 and Alessio Ciulli for providing the VCB expression vectors. We thank HZB for the allocation of synchrotron radiation beamtime and we would particularly like to acknowledge the help and support of Manfred Weiss and the whole MX team during the experiment.^[33] This work was supported by the NewPRO project of the PROXIDRUGS consortium (03ZU1109FD), the DFG grants HA-5565-5/1 and 461372424 as well as by the LOEWE project TRABITA. E.M. was funded during the course of this work through a Humboldt Forschungstipendium (Alexander von Humboldt Stiftung). Open Access funding enabled and organized by Projekt DEAL.

Conflict of Interest

The authors declare no conflict of interest.

Data Availability Statement

The data that support the findings of this study are available in the supplementary material of this article.

Keywords: FKBP · FKBP51 · Glucocorticoid Receptor · Proteolysis Targeting Chimeras (PROTACs) · Targeted Protein Degradation

- [1] a) V. Némec, M. P. Schwalm, S. Müller, S. Knapp, *Chem. Soc. Rev.* **2022**, *51*, 7971; b) M. Békés, D. R. Langley, C. M. Crews, *Nat. Rev. Drug Discovery* **2022**, *21*, 181.
- [2] X. Yu, D. Li, J. Kottur, Y. Shen, H. S. Kim, K.-S. Park, Y.-H. Tsai, W. Gong, J. Wang, K. Suzuki, J. Parker, L. Herring, H. Ü. Kaniskan, L. Cai, R. Jain, J. Liu, A. K. Aggarwal, G. G. Wang, J. Jin, *Sci. Transl. Med.* **2021**, *13*, eabj1578.
- [3] R. P. Law, J. Nunes, C.-W. Chung, M. Bantscheff, K. Buda, H. Dai, J. P. Evans, A. Flinders, D. Klimaszewska, A. J. Lewis, M. Muelbaier, P. Scott-Stevens, P. Stacey, C. J. Tame, G. F. Watt, N. Zinn, M. A. Queisser, J. D. Harling, A. B. Benowitz, *Angew. Chem. Int. Ed.* **2021**, *60*, 23327.
- [4] W. Farnaby, M. Koegl, M. J. Roy, C. Whitworth, E. Diers, N. Trainor, D. Zollman, S. Steurer, J. Karolyi-Oezguer, C. Riedmueller, T. Gmaschitz, J. Wachter, C. Dank, M. Galant, B. Sharps, K. Rumpel, E. Traxler, T. Gerstberger, R. Schnitzer, O. Petermann, P. Greb, H. Weinstabl, G. Bader, A. Zoephel, A. Weiss-Puxbaum, K. Ehrenhöfer-Wölfer, S. Wöhrle, G. Boehmelt, J. Rinnenthal, H. Arnhof, N. Wiechens, M.-Y. Wu, T. Owen-Hughes, P. Ettmayer, M. Pearson, D. B. McConnell, A. Ciulli, *Nat. Chem. Biol.* **2019**, *15*, 672.
- [5] B. Adhikari, J. Bozilovic, M. Diebold, J. D. Schwarz, J. Hofstetter, M. Schröder, M. Wanior, A. Narain, M. Vogt, N. Dudvarski Stankovic, A. Baluapuri, L. Schönemann, L. Eing, P. Bhandare, B. Kuster, A. Schlosser, S. Heinzlmeir, C. Sottriffer, S. Knapp, E. Wolf, *Nat. Chem. Biol.* **2020**, *16*, 1179.
- [6] a) A. Baischew, S. Engel, T. M. Geiger, M. C. Taubert, F. Hausch, *J. Cell. Biochem.* **2023**, <https://doi.org/10.1002/jcb.30384>; b) O. B. Soto, C. S. Ramirez, R. Koyani, I. A. Rodriguez-Palomares, J. R. Dirmeyer, B. Grajeda, S. Roy, M. B. Cox, *J. Cell. Biochem.* **2023**, <https://doi.org/10.1002/jcb.30406>; c) N. T. Gebru, S. E. Hill, L. J. Blair, *J. Cell. Biochem.* **2023**, <https://doi.org/10.1002/jcb.30374>; d) N. M. Galigniana, M. C. Ruiz, G. Piwien-Pilipuk, *J. Cell. Biochem.* **2022**, <https://doi.org/10.1002/jcb.30351>.
- [7] a) E. R. Sanchez, *Biochim. Biophys. Acta* **2012**, *1823*, 722; b) C. L. Storer, C. A. Dickey, M. D. Galigniana, T. Rein, M. B. Cox, *Trends Endocrinol. Metab.* **2011**, *22*, 481.
- [8] a) J. C. O'Leary, S. Dharra, L. J. Blair, S. Brady, A. G. Johnson, M. Peters, J. Cheung-Flynn, M. B. Cox, G. de Erausquin, E. J. Weeber, U. K. Jinwal, C. A. Dickey, *PLoS One* **2011**, *6*, e24840; b) C. Touma, N. C. Gassen, L. Herrmann, J. Cheung-Flynn, D. R. Büll, I. A. Ionescu, J.-M. Heinzmann, A. Knapman, A. Siebertz, A.-M. Depping, J. Hartmann, F. Hausch, M. V. Schmidt, F. Holsboer, M. Ising, M. B. Cox, U. Schmidt, T. Rein, *Biol. Psychiatry* **2011**, *70*, 928; c) S. Albu, C. P. N. Romanowski, M. Letizia Curzi, V. Jakubcakova, C. Flachskamm, N. C. Gassen, J. Hartmann, M. V. Schmidt, U. Schmidt, T. Rein, F. Holsboer, F. Hausch, M. Paez-Pereda, M. Kimura, *J. Sleep Res.* **2014**, *23*, 176.
- [9] J. Hartmann, K. V. Wagner, C. Liebl, S. H. Scharf, X.-D. Wang, M. Wolf, F. Hausch, T. Rein, U. Schmidt, C. Touma, J. Cheung-Flynn, M. B. Cox, D. F. Smith, F. Holsboer, M. B. Müller, M. V. Schmidt, *Neuropharmacology* **2012**, *62*, 332.
- [10] S. D. Linnstaedt, K. D. Riker, C. A. Rueckeis, K. M. Kutchko, L. Lackey, K. R. McCarthy, Y.-H. Tsai, J. S. Parker, M. C.

- Kurz, P. L. Hendry, C. Lewandowski, E. Datner, C. Pearson, B. O'Neil, R. Domeier, S. Kaushik, A. Laederach, S. A. McLean, *J. Neurosci.* **2018**, *38*, 8407.
- [11] B. J. Wanstrath, S. A. McLean, Y. Zhao, J. Mickelson, M. Bauder, F. Hausch, S. D. Linnstaedt, *J. Pain* **2022**, *23*, 1256.
- [12] S. Wedel, P. Mathoor, O. Rauh, T. Heymann, C. I. Ciotu, D. C. Fuhrmann, M. J. M. Fischer, A. Weigert, N. de Bruin, F. Hausch, G. Geisslinger, M. Sisignano, *J. Neuroinflammation* **2022**, *19*, 254.
- [13] M. Maiarù, O. B. Morgan, T. Mao, M. Breitsamer, H. Bamber, M. Pöhlmann, M. V. Schmidt, G. Winter, F. Hausch, S. M. Géranton, *Pain* **2018**, *159*, 1224.
- [14] G. Balsevich, A. S. Häusl, C. W. Meyer, S. Karamihalev, X. Feng, M. L. Pöhlmann, C. Dournes, A. Uribe-Marino, S. Santarelli, C. Labermaier, K. Hafner, T. Mao, M. Breitsamer, M. Theodoropoulou, C. Namendorf, M. Uhr, M. Paez-Pereda, G. Winter, F. Hausch, A. Chen, M. H. Tschöp, T. Rein, N. C. Gassen, M. V. Schmidt, *Nat. Commun.* **2017**, *8*, 1725.
- [15] M. J. Pereira, J. Palming, M. K. Svensson, M. Rizell, J. Dalenbäck, M. Hammar, T. Fall, C. O. Sidibeh, P.-A. Svensson, J. W. Eriksson, *Metabolism* **2014**, *63*, 1198.
- [16] C. O. Sidibeh, M. J. Pereira, X. M. Abalo, G. J. Boersma, S. Skrtic, P. Lundkvist, P. Katsogiannos, F. Hausch, C. Castillejo-López, J. W. Eriksson, *Endocrine* **2018**, *62*, 116.
- [17] K. B. Smedlund, E. R. Sanchez, T. D. Hinds, *Trends Endocrinol. MeTable* **2021**, *32*, 862.
- [18] A. Baischew, S. Engel, M. C. Taubert, T. M. Geiger, F. Hausch, *Nat. Struct. Mol. Biol.* **2023**, *30*, 1857-1866 <https://doi.org/10.1038/s41594-023-01098-1>.
- [19] C. M. Noddings, J. L. Johnson, D. A. Agard, *Nat. Struct. Mol. Biol.* **2023**, *30*, 1867-1877 <https://doi.org/10.1038/s41594-023-01128-y>.
- [20] a) S. Gaali, A. Kirschner, S. Cuboni, J. Hartmann, C. Kozany, G. Balsevich, C. Namendorf, P. Fernandez-Vizarrá, C. Sippel, A. S. Zannas, R. Draenert, E. B. Binder, O. F. X. Almeida, G. Rühler, M. Uhr, M. V. Schmidt, C. Touma, A. Bracher, F. Hausch, *Nat. Chem. Biol.* **2015**, *11*, 33; b) F. H. Knaup, C. Meyners, W. O. Sugiarto, S. Wedel, M. Springer, C. Walz, T. M. Geiger, M. Schmidt, M. Sisignano, F. Hausch, *J. Med. Chem.* **2023**, *66*, 5965; c) A. M. Voll, C. Meyners, M. C. Taubert, T. Bajaj, T. Heymann, S. Merz, A. Charalampidou, J. Kolos, P. L. Purder, T. M. Geiger, P. Wessig, N. C. Gassen, A. Bracher, F. Hausch, *Angew. Chem. Int. Ed.* **2021**, *60*, 13257.
- [21] M. Bauder, C. Meyners, P. L. Purder, S. Merz, W. O. Sugiarto, A. M. Voll, T. Heymann, F. Hausch, *J. Med. Chem.* **2021**, *64*, 3320.
- [22] S. Pomplun, Y. Wang, A. Kirschner, C. Kozany, A. Bracher, F. Hausch, *Angew. Chem. Int. Ed.* **2015**, *54*, 345.
- [23] S. Pomplun, C. Sippel, A. Hähle, D. Tay, K. Shima, A. Klages, C. M. Ünal, B. Rieß, H. T. Toh, G. Hansen, H. S. Yoon, A. Bracher, P. Preiser, J. Rupp, M. Steinert, F. Hausch, *J. Med. Chem.* **2018**, *61*, 3660.
- [24] J. M. Kolos, S. Pomplun, S. Jung, B. Rieß, P. L. Purder, A. M. Voll, S. Merz, M. Gnatzy, T. M. Geiger, I. Quist-Løkken, J. Jatzlau, P. Knaus, T. Holien, A. Bracher, C. Meyners, P. Czodrowski, V. Krewald, F. Hausch, *Chem. Sci.* **2021**, *12*, 14758.
- [25] M. S. Gadd, A. Testa, X. Lucas, K.-H. Chan, W. Chen, D. J. Lamont, M. Zengerle, A. Ciulli, *Nat. Chem. Biol.* **2017**, *13*, 514.
- [26] a) V. Zoppi, S. J. Hughes, C. Maniaci, A. Testa, T. Gmaschitz, C. Wieshofer, M. Koegl, K. M. Ricking, D. L. Daniels, A. Spallarossa, A. Ciulli, *J. Med. Chem.* **2019**, *62*, 699; b) K. M. Ricking, J. D. Vasta, S. J. Hughes, V. Zoppi, C. Maniaci, A. Testa, M. Urh, A. Ciulli, D. L. Daniels, *Curr. Res. Chem. Biol.* **2021**, *1*, 100009.
- [27] Z. Kozicka, N. H. Thomä, *Cell Chem. Biol.* **2021**, *28*, 1032.
- [28] T. Mathieson, H. Franken, J. Kosinski, N. Kurzawa, N. Zinn, G. Sweetman, D. Poeckel, V. S. Ratnu, M. Schramm, I. Becher, M. Steidel, K.-M. Noh, G. Bergamini, M. Beck, M. Bantscheff, M. M. Savitski, *Nat. Commun.* **2018**, *9*, 689.
- [29] M. V. Schmidt, M. Paez-Pereda, F. Holsboer, F. Hausch, *ChemMedChem* **2012**, *7*, 1351.
- [30] M. Maiarù, K. K. Tochiki, M. B. Cox, L. V. Annan, C. G. Bell, X. Feng, F. Hausch, S. M. Géranton, *Sci. Transl. Med.* **2016**, *8*, 325ra19.
- [31] M. Kästle, B. Kistler, T. Lamla, T. Bretschneider, D. Lamb, P. Nicklin, D. Wyatt, *Eur. J. Immunol.* **2018**, *48*, 1904.
- [32] a) J. Krieger, F. J. Sorrell, A. A. Wegener, B. Leuthner, F. Machrouhi-Porcher, M. Hecht, E. M. Leibrock, J. E. Müller, J. Eisert, I. V. Hartung, S. Schlesiger, *ChemMedChem* **2023**, *18*, e202200615; b) X. Liu, A. F. Kalogeropoulou, S. Domingos, N. Makukhin, R. S. Nirujogi, F. Singh, N. Shpiro, A. Saalfrank, E. Sammler, I. G. Ganley, R. Moreira, D. R. Alessi, A. Ciulli, *J. Am. Chem. Soc.* **2022**, *144*, 16930; c) C. Kofink, N. Trainor, B. Mair, S. Wöhrle, M. Wurm, N. Mischerikow, M. J. Roy, G. Bader, P. Greb, G. Garavel, E. Diers, R. McLennan, C. Whitworth, V. Vetma, K. Rumpel, M. Scharnweber, J. E. Fuchs, T. Gerstberger, Y. Cui, G. Gremel, P. Chetta, S. Hopf, N. Budano, J. Rinnenthal, G. Gmaschitz, M. Mayer, M. Koegl, A. Ciulli, H. Weinstabl, W. Farnaby, *Nat. Commun.* **2022**, *13*, 5969; d) C.-W. Chung, H. Dai, E. Fernandez, C. P. Tinworth, I. Churcher, J. Cryan, J. Denyer, J. D. Harling, A. Konopacka, M. A. Queisser, C. J. Tame, G. Watt, F. Jiang, D. Qian, A. B. Benowitz, *ACS Chem. Biol.* **2020**, *15*, 2316; e) A. Testa, S. J. Hughes, X. Lucas, J. E. Wright, A. Ciulli, *Angew. Chem. Int. Ed.* **2020**, *59*, 1727; f) A. Hanzl, R. Casement, H. Imrichova, S. J. Hughes, E. Barone, A. Testa, S. Bauer, J. Wright, M. Brand, A. Ciulli, G. E. Winter, *Nat. Chem. Biol.* **2023**, *19*, 323.
- [33] M. Gerlach, U. Mueller, M. S. Weiss, *JLSRF* **2016**, *2*, A47.

Manuscript received: August 21, 2023

Accepted manuscript online: November 9, 2023

Version of record online: December 14, 2023